The set of triple-resonance sequences with a multiple quantum coherence evolution period

Wiktor Koźmiński[a,*], Igor Zhukov[b]

[a] *Department of Chemistry, Warsaw University, ul. Pasteura 1, 02-093 Warszawa, Poland*
[b] *Institute of Biochemistry and Biophysics, Polish Academy of Sciences, ul. Pawińskiego 5a, 02-106 Warszawa, Poland*

Abstract

The new pulse sequence building block that relies on evolution of heteronuclear multiple quantum coherences is proposed. The particular chemical shifts are obtained in multiple quadrature, using linear combinations of frequencies taken from spectra measured at different quantum levels. The pulse sequences designed in this way consist of small number of RF-pulses, are as short as possible, and could be applied for determination of coupling constants. The examples presented involve 2D correlations HNCO, HNCA, HN(CO)CA, and H(N)COCA via heteronuclear zero and double coherences, as well as 2D HNCOCA technique with simultaneous evolution of triple and three distinct single quantum coherences. Applications of the new sequences are presented for ^{13}C,^{15}N-labeled ubiquitin.
© 2004 Elsevier Inc. All rights reserved.

Keywords: HNCO; HNCA; HN(CO)CA; H(N)COCA; HNCOCA; Multiple quantum evolution; Reduced dimensionality; Sequential assignment; Triple resonance; Coupling constants; Ubiquitin

1. Introduction

The introduction of 2D NMR techniques [1,2] has created new possibilities in applications of NMR spectroscopy in chemistry and biochemistry. The acquisition of multidimensional data sets allows one to correlate several different chemical shifts, and to separate degenerated signals by spreading them in different frequency domains. However, the possible digital resolution is strongly limited by the acceptable experimental time. The most important course of this limitation, directly relating the experimental time to the achievable resolution, is the necessity of acquiring large quantity of data sets. The number of these sets is proportional to the product of the number of data points in all indirectly detected time domains.

Recently, a number of new ideas accelerating the acquisition of multidimensional data sets have been proposed. The new approaches involve: spatially encoded chemical shift evolution followed by spatially resolved acquisition [3–6], reconstruction of multidimensional spectra from sets of projections [7–10], and new variants of reduced dimensionality (RD) techniques [11–13]. These recently introduced RD experiments employ either TPPI for signal displacement [14] or a multiple quadrature variant [15–17] for elucidation of single frequencies.

The general idea of RD-methods, analogously to the concept of Accordion spectroscopy [18,19], involves simultaneous sampling of two or more chemical shifts evolutions. Thus, the N chemical shifts could be effectively encoded in M-dimensional spectrum ($2 \leqslant M \leqslant N - 1$). However, for full exploration of the advantages

of RD-type experiments, i.e., short measurement times and resolution limited only by apparent transverse relaxation rates, determination of sign (with respect to carrier offset) of all simultaneously sampled frequencies requires the application of a multiple quadrature [15–17]. The multiple quadrature effect could be easily achieved by extension of the known rules of quadrature detection, i.e., by acquisition and appropriate combination of sine and cosine amplitude or echo and antiecho phase modulated data sets for each involved frequency. Thus, for the n frequencies in a common domain, the acquisition and appropriate coaddition of 2^n FIDs per each t_1 increment is necessary, producing a set of spectra with 2^n possible sign combinations of particular frequencies. The 2^{n-1} relevant combinations form a system of independent linear equations, the solving of which allows the recovery of full chemical shift information. Additionally, the number of spectra which can be generated from acquired data (2^{n-1}) increases faster than the number of combined frequencies. Thus, for three frequencies in a single dimension four independent, out of eight possible combinations of the frequency signs are available. Hence, there are four linear equations describing three unknowns, and eight equations for four unknowns for $n = 4$. Therefore, the precision of obtained chemical shifts could be significantly improved by simple averaging (i.e., for three spins A, B, and C, each particular resonance frequency could be evaluated as an average from signal frequencies obtained from three different sets of four subspectra with $+\Omega_A \pm \Omega_B \pm \Omega_C$, $\pm \Omega_A + \Omega_B \pm \Omega_C$, and $\pm \Omega_A \pm \Omega_B + \Omega_C$, respectively). Since the cross-peak displacements in all the independent spectra are, in general, different, the same peaks could be overlapping in one spectrum while separated in the others, still enabling a full analysis. In a single quadrature RD-experiments [11–14] frequency offset for the nuclei detected without quadrature should be set outside of its spectral region, thus increasing number of necessary time domain points. Multiple quadrature detection not only clarifies the spectrum by 2-fold reduction of the number of peaks for each frequency in the RD-domain, but also allows decreasing of the sampled frequency range, by setting the transmitter offsets at the center of regions of interest. The implementation of this technique in the existing pulse-sequences is straightforward, and simply requires equal or mutually proportional setting of all evolution times, while retaining all statements responsible for quadrature in the indirectly detected domains. A suitable processing scheme, providing spectra with all possible combination of frequency signs (i.e., $\pm \Omega_A \pm \Omega_B \pm \Omega_C$), is described in our previous communication [16].

In the present work, we propose a new set of techniques optimized for RD-type acquisition by the use of a single MQ-coherences evolution period. We also demonstrate that application of the same processing procedure as for the standard RD-spectra could be employed for elucidating single frequencies. Although we have already applied a DQ/ZQ H_α–C_α evolution period in the HACANH technique [16], until now most of the RD-sequences were derived directly from their multidimensional versions. MQ-evolution period has been also used for simultaneous sampling of two frequencies in HN(CO)CACB, HN(COCA)CACB, HN(CO)CAHA, and HN(COCA)CACB sequences [14], however, in this case a TPPI method was employed to distinguish different peaks, instead of the multiple quadrature. The spectra obtained using MQ-evolution periods are similar to those acquired using several simultaneously incremented evolution periods; for example, the 2D RD-spectra acquired using sequences with two separate single quantum evolution periods, shown in [15], are also by analogy called zero and double quantum. Employing a single t_1 period results in evolution of true multiple quantum coherences. Moreover, pulse sequences designed in this way consist of a small number of RF-pulses and are as short as possible. Recently, a similar concept of multiple quantum RD-evolution has been applied to magic angle spinning experiment in solid state NMR of biomolecules [20].

2. Results and discussion

The pulse sequence schemes for the proposed experiments are depicted in Figs. 1 and 2. All of them employ out-and-back coherence transfer with excitation and detection of H_N protons, and are characterized by a single t_1 evolution period. The sequences obtained by the combination of a general scheme (Fig. 1A) with the central elements (Figs. 1B–E) give the MQ variants of HNCA, HNCO, HN(CO)CA, and HNCOCA experiments, respectively. The sensitivity enhancement detection [21–23] introduces ^{15}N phase modulation in t_1, while $^{13}C_\alpha/^{13}C'$ evolution causes amplitude modulations. In the H(N)COCA experiment (Fig. 2A), characterized by the lack of a ^{15}N chemical shift evolution, purely t_1-amplitude modulated data sets are being acquired.

The characteristic feature of the proposed experiments is replacement of polarization transfers in INEPT manner by nested HMQC building blocks. Only in H(N)COCA (Fig. 2A) the N–C INEPT is used. The t_1 period is placed at the central point of the sequence, and directly after it the evolution is refocused in such a way that the effective evolution time of transverse magnetization is equal either to t_1 for coherences of interest or to zero. Since we have used a spectrometer equipped with a single ^{13}C RF-channel, to avoid breaking the phase coherence by frequency changes, the ^{13}C carrier offset was constant for the whole duration of pulse sequences [24]. It was set to the center of $^{13}C'$
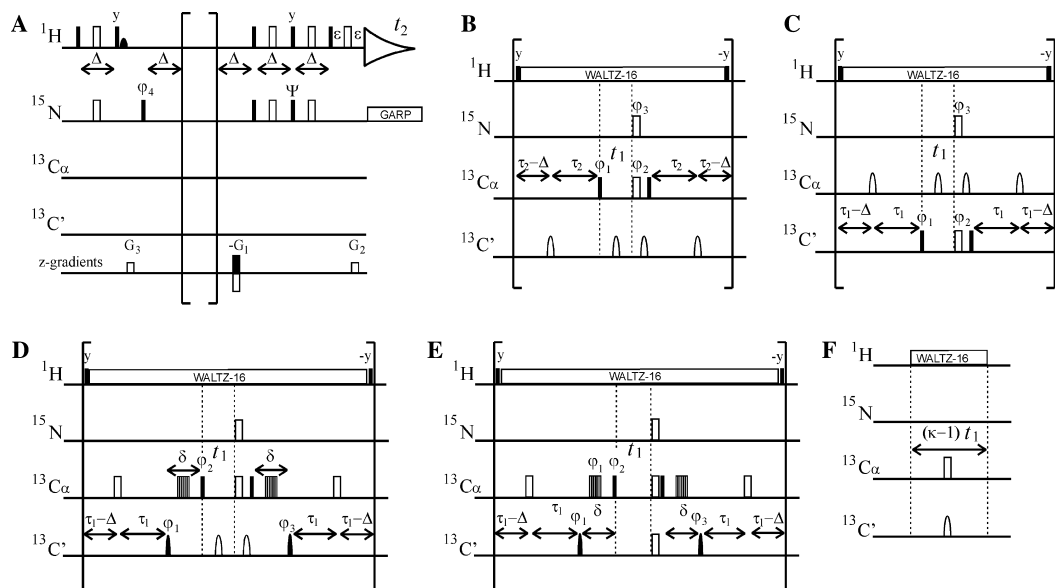
Fig. 1. Pulse sequences of the reduced dimensionality multiple quantum experiments. (A) General, with sensitivity enhancement, scheme for out and back experiments involving H_N nuclei, (A) + (B) H<u>NCA</u>, (A) + (C) H<u>NCO</u>, (A) + (D) H<u>N(CO)CA</u>, (A) + (E) H<u>NCOCA</u>, and (F) element for relative scaling up of a ^{15}N chemical shift evolution by factor of κ. Dark-filled and open bars represent $\pi/2$ and π pulses, respectively. The selective rectangular pulses are applied on resonance with γB_1 set to $\Delta\Omega/\sqrt{15}$ and $\Delta\Omega/\sqrt{3}$ for $\pi/2$ and π pulses, respectively, where $\Delta\Omega$ is a difference between centers of C′ and C_α spectral regions. Off resonance pulses are realized using linear phase modulated sinc shapes. Water flip-back was applied as a sinc-shaped pulse of 2.1 ms duration, in the initial INEPT step. For all sequences, except H<u>NCO</u> (A) + (C), the ^{13}C carrier offset was set to the center of the C_α region (56 ppm). Thus, for H<u>NCOCA</u> sequence (A) + (E), involving simultaneous ^{15}N, $^{13}C′$, and $^{13}C_\alpha$ chemical shift evolution, TPPI in steps of $-360\Delta\Omega/(2\pi SW1)$ degrees was added to ϕ_1 to shift the center of the C′ signal region by -118 ppm, where SW1 is the F_1 spectral width. For efficient simultaneous inversion of $^{13}C_\alpha$ and refocusing of $^{13}C′$ spins the six-element composite pulses [32] were employed. All pulses were applied along the rotating-frame x-axis unless indicated differently. The delays Δ should be tuned to $0.5/^1J(^{15}N, ^1H)$. $2\tau_1$ and $2\tau_2$ (28 and 22 ms) were optimized for maximum amplitude of polarization transfer between ^{13}C and ^{15}N, and δ was set to 7 ms. ϵ includes the rectangular-shaped gradient pulse and a 100 μs recovery time. All delays are carefully matched regarding pulse widths to obtain zero phase corrections for the coherences of interest. The basic phase cycles are: for sequences (A) + (B,C) $\phi_1 = x, -x$, $\phi_2 = x, y, -x, -y$, $\phi_3 = 8x, 8y, 8(-x)8(-y)$, $\phi_4 = 4x, 4(-x)$, and $\phi_R = \phi_1 + 2\phi_2 + 2\phi_3 + \phi_4$, whereas for (A) + (D,E) $\phi_1 = x, -x$, $\phi_2 = x, -x$, $\phi_3 = 4x, 4(-x)$, $\phi_4 = 8x, 8(-x)$, and $\phi_R = \phi_1 + \phi_2 + \phi_3 + \phi_4$. ^{15}N quadrature was obtained using echo-antiecho PFG-selection by G_1 and G_2 gradients with duration of 1 ms, and the relative amplitude of $\pm\gamma_H/\gamma_N$, with phase ψ set to $-\pi/2$ in echo, and $+\pi/2$ in antiecho experiments, respectively. $^{13}C_\alpha$ and $^{13}C′$ quadratures were obtained by $\pi/2$ phase shifts of ϕ_1 [33]. The quadrature detection requires acquisition of four data sets per each t_1 increment for formally 3D sequences (A) + (B–D), whereas for formally 4D H<u>NCOCA</u> experiment (A) + (E), eight independent data sets per each t_1 value should be collected. The axial peaks were displaced by simultaneous reversing of the sign of ϕ_1 and receiver phase (ϕ_R) for the even t_1 increments [34].

region (176 ppm) in H<u>NCO</u> (Figs. 1A and C), whereas to 56 ppm in others. For this reason the usual off resonance $^{13}C_\alpha/^{13}C′$ linearly phase modulated sinc pulses were applied. For the H(N)<u>COCA</u> (Fig. 2A) and H<u>NCOCA</u> (Figs. 1A and E) sequences, where multiple quantum coherences involving $^{13}C_\alpha$ and $^{13}C′$ evolve with carrier offset in the middle of the $^{13}C_\alpha$ region, a standard procedure would require a very large spectral range. Hence, we decided to use the TPPI [25,26] incrementation of ϕ_1 with a phase shift of $-360\Delta\Omega/(2\pi SW1)$ degrees. ($\Delta\Omega/2\pi$ is the difference between $^{13}C′$ and $^{13}C_\alpha$ spectral region centers (118 ppm) and SW1 actual spectral width in indirectly detected dimension). Thus, the effective $^{13}C′$ and $^{13}C_\alpha$ spectral regions were centered at the middle of the F_1 dimension, allow the use of minimal necessary SW1. Since active coupling does not evolve for MQ-coherences, only couplings involving passive spins need to be refocused in the t_1, which simplifies the pulse sequences.

Application of the multiple quadrature, which is essential for evaluation of single quantum frequencies, requires interleaved acquisition of an array of four data sets for DQ/ZQ sequences (Figs. 1A and B–D) and (Fig. 2A). However, formally 4D H<u>NCOCA</u> experiment (Figs. 1A and E) encoding three frequencies in a common domain, requires the acquisition of eight data sets per each t_1 increment. The appropriate processing scheme has already been comprehensively described [16], and relies on coaddition of a cosine and sine amplitude modulated data sets with $\pm\pi/2$ phase correction of the latter in t_1.

In case of several simultaneously sampled evolution periods, the application of relative scaling of evolution increments is straightforward and allows for optimization of spectral resolution with regard to transverse relaxation rates. For the MQ-sequences proposed in the present work, it is still possible to scale up the ^{15}N evolution by factor of κ. It simply requires insertion of the element Fig. 1F, prior to the first ^{13}C $\pi/2$ pulse.
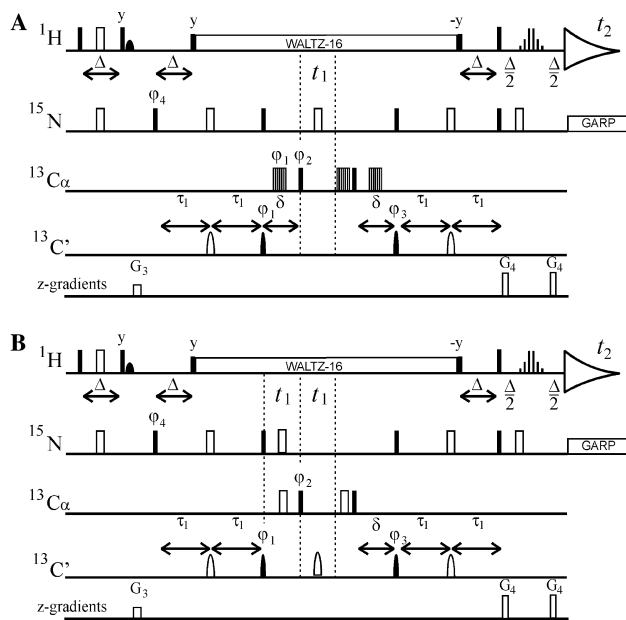
Fig. 2. Pulse sequences for reduced dimensionality H(N)COCA experiments. (A) Pulse sequence with single DQ/ZQ evolution period, (B) technique with separate evolution periods, according to [24]. In both cases the ^{13}C carrier offset was set to the center of the ^{13}C$_\alpha$ region (56 ppm), and TPPI in steps of $-360\Delta\Omega/(2\pi\text{SW1})$ degrees was added to ϕ_1 to shift the center of the C$'$ signal region by -118 ppm, where SW1 is the F_1 spectral width. Additionally, the BSP correction was added to ϕ_3. The phase cycle applied was: $\phi_1 = x, -x$, $\phi_2 = x, -x$, $\phi_3 = 4x, 4(-x)$, $\phi_4 = 8x, 8(-x)$, and $\phi_R = \phi_1 + \phi_2 + \phi_3 + \phi_4$. Water signal suppression was accomplished by PFG-spin-echo with 3-9-19 refocusing element in reverse INEPT step. ^{13}C$_\alpha$ and ^{13}C$'$ quadratures were obtained by $\pi/2$ phase shifts of ϕ_1 and ϕ_2 [33]. Because of lack of ^{15}N chemical shift evolution we modified original H(N)COCA sequence [24], replacing heteronuclear PFG echo with sensitivity enhancement ^{15}N–^{1}H coherence transfer by simple inverse INEPT with water signal suppression (see above).

The spectrum obtained using MQ-HNCO sequence is shown in Figs. 3A and B. The peak frequencies in double quantum spectra (Fig. 3A) are equal to the sum of respective ^{15}N and ^{13}C$'$ frequencies, whereas in zero quantum spectra (Fig. 3B) the difference of frequencies is observed. The spectra containing information about C$_\alpha$ chemical shifts, obtained using the MQ-versions of HNCA, HN(CO)CA, and H(N)COCA, are plotted in Fig. 4. Similarly as in Fig. 3 the DQ-spectra are located in the left column (A,C,E) and ZQ in the right one (B,D,F). Fig. 5 shows the results of application of a formally 4D experiment HNCOCA, correlating amide proton resonances with ^{15}N, ^{13}C$'$, and ^{13}C$_{\alpha(i-1)}$ in a single experiment. In this case triple spin coherences are created and evolve over t_1. Thus, the triple and three distinct single quantum spectra could be obtained with all possible combinations of frequency signs. This experiment exhibits good sensitivity and signal dispersion.

In Fig. 3 the spectra are presented with positive sign of ^{15}N frequencies combined with positive and negative signs of ^{13}C$'$ displacement. However, for the spectra
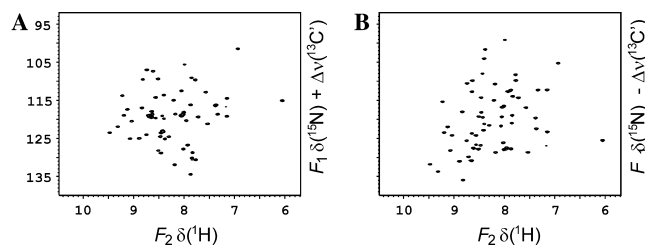

Fig. 3. Contour plots of two-dimensional spectra obtained using reduced dimensionality 2D HNCO sequence from Figs. 1A and C applied to ^{13}C, ^{15}N-labeled ubiquitin sample. (A and B) Plots show double and zero quantum spectra, respectively. The time-domain data were processed, according to previously published procedure [16] with retention of positive ^{15}N frequencies. The signal frequency in F_1 domain is equal to $\delta(^{15}\text{N}) \pm \Delta v(^{13}\text{C}')$, where $\Delta v(^{13}\text{C}')$ denotes frequency differences between ^{13}C$'$ resonance and carrier offset. Sixteen scans were coherently added for each data set for 256 t_1 increments. The maximum t_1 and t_2 times were 85 and 102 ms, respectively. The spectral width of 3000 Hz, covering the sum of ^{15}N and ^{13}C$'$ spectral ranges, was set for the F_1 dimension. A relaxation delay of 1.5 s was used. The data matrix containing 256×512 complex points in t_1 and t_2, respectively, was zero-filled to 1024×1024 complex points. Cosine square weighting function was applied prior to Fourier transformation in both dimensions.
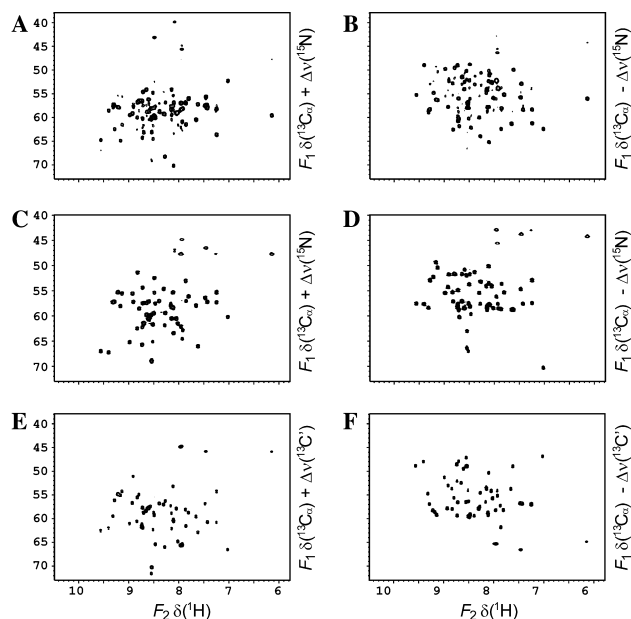

Fig. 4. Contour plots obtained by application of the HNCA (A and B), HN(CO)CA (C and D), and H(N)COCA (E and F), pulse sequences from Figs. 1(A and B), (A and D), and 2A, respectively to ^{13}C, ^{15}N-labeled ubiquitin sample. The signal coordinates in F_1 dimension of DQ- (A, C, and E) and ZQ-spectra (B, D, and F) are equal to the sum and differences of involved frequencies, respectively. The data were processed according to [16], with retention of positive ^{13}C$_\alpha$ frequencies, common in all spectra. Sixteen scans were coherently added for each data set for 192 t_1 increments. The maximum t_1 and t_2 times were 36 and 102 ms, respectively. The spectral width of 5400 Hz, covering the sum of ^{15}N, ^{13}C$_\alpha$, and ^{13}C$'$ spectral ranges, was set for the F_1 dimension. A relaxation delay of 1.4 s was used. The data matrix containing 192×512 complex points in t_1 and t_2, respectively, was zero-filled to 1024×1024 complex points. Cosine square weighting function was applied in both dimensions prior to Fourier transformation.
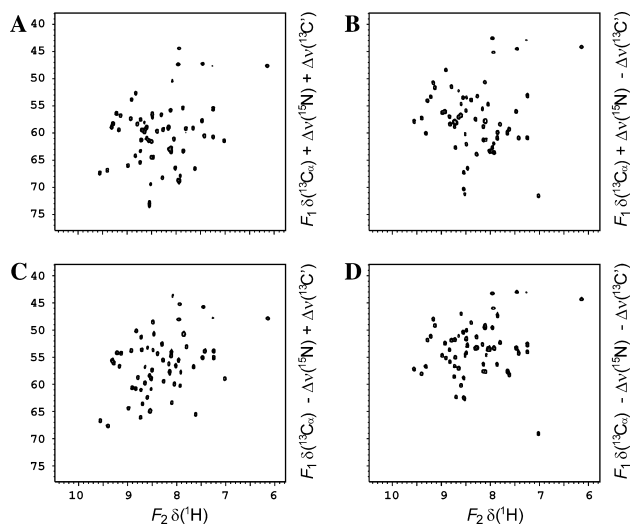
Fig. 5. Contour plots obtained by application of the HNCOCA pulse sequence from Figs. 1A and E, to ^{13}C, ^{15}N-labeled ubiquitin sample. (A) TQ-spectrum and (B–D) three distinct SQ-spectra with different sign combination of ^{15}N and ^{13}C frequencies. The data were processed with retention positive sign of ^{13}C$_\alpha$ frequency [16]. Sixteen scans were coherently added to each data set for 192 t_1 increments. The maximum t_1 and t_2 times were 36 and 102 ms, respectively. The spectral width of 5400 Hz, covering the sum of ^{15}N, ^{13}C$_\alpha$, and ^{13}C′ spectral ranges, was set for the F_1 dimension. A relaxation delay of 1.5 s was used. The data matrix containing 192 × 512 complex points in t_1 and t_2, respectively, was zero-filled to 1024 × 1024 complex points. Cosine square weighting function was applied prior to Fourier transformation in both dimensions.

shown in Figs. 4 and 5, we decided to retain the positive sign of ^{13}C$_\alpha$ frequencies since they are common for all four experiments. Therefore, in Fig. 3 peaks are centered around the ^{15}N frequency, whereas in Figs. 4 and 5— around ^{13}C$_\alpha$ one. Different arrangements of the spectra are also possible by straightforward data manipulation [16].

The sensitivity of the new multiple quantum version of the HNCO and H(N)COCA sequences should be related to their known variants with single quantum evolution periods. The comparison of F_1 cross sections across amide resonance of Leu67 is shown in Fig. 6. Trace (A) is obtained by application of standard 2D HNCO, with INEPT transfer between ^{15}N and ^{13}C′ nuclei and single quantum evolution periods, acquired in reduced dimensionality manner. The maximum t_1 was limited by constant-time ^{15}N chemical shift evolution to ca. 28 ms. Trace (B) was recorded using DQ/ZQ 2D HNCO from Figs. 1A and C, using the same acquisition parameters. There is no significant difference in signal-to-noise ratio. To show ability of DQ/ZQ 2D HNCO (Figs. 1A and C) to acquire spectra with longer evolution time t_1, we show trace (C) which is extracted from spectrum obtained in the same experimental time as (A and B), but with doubled number of t_1 increments and halved number of accumulations. The line width is almost 2-fold reduced with slight decrease of S/N
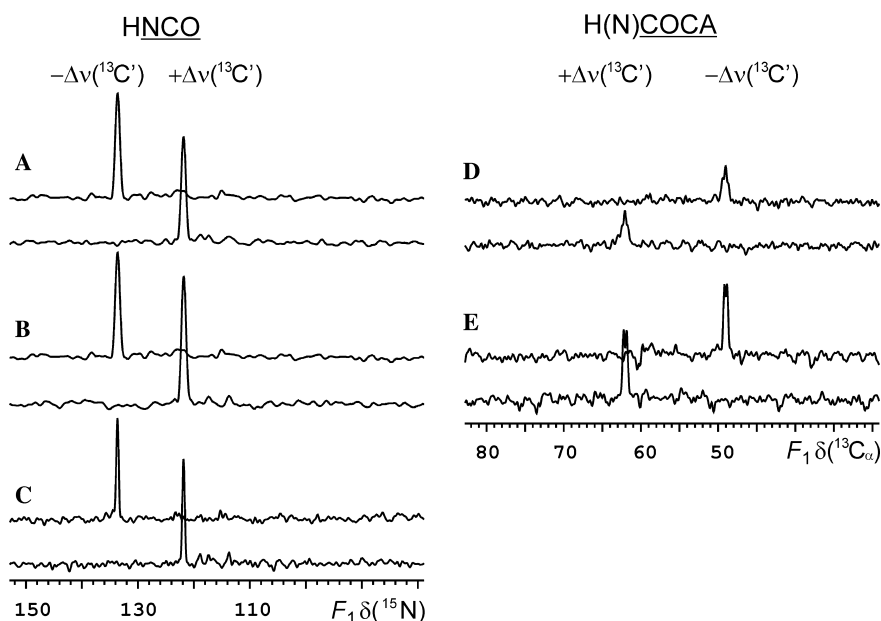

Fig. 6. Comparison of the F_1 cross sections across amide resonance of Leu67 residue. (A) Conventional 2D reduced dimensionality HNCO with INEPT transfer between ^{15}N and ^{13}C′ nuclei and constant-time ^{15}N chemical shift evolution, 16 scans added for each data set for 83 t_1 increments (the maximum t_1 was 27.7 ms). (B) 2D reduced dimensionality HNCO acquired using sequence from Figs. 1A and C, acquisition parameters as above. (C) The same sequence as in (B) but recorded with eight scans added for each data set and 166 t_1 increments (the maximum t_1 was 55.3 ms). (D) 2D reduced dimensionality H(N)COCA spectrum obtained by application of sequence from Fig. 2B [24], and (E) H(N)COCA spectrum acquired using sequence from Fig. 2A with single DQ/ZQ period. For traces (D and E) identical acquisition parameters were used (see caption to Fig. 4). The signal frequencies in upper and lower traces represent spectra with difference and sum of the involved frequencies, respectively. Traces (A and D) represent doubly modulated single quantum spectra, while (B, C, and E) are examples of zero- and double quantum experiments.

due to transverse relaxation in longer t_1 period. The conventional HNCO would require for this t_1 two separate $^{13}C'$ and ^{15}N evolution periods. It should be noted, however, that at the higher B_0 fields significant extending of t_1 evolution in DQ/ZQ 2D H<u>NCO</u>, would be limited by effective chemical shift anisotropy relaxation of $^{13}C'$ nuclei. Similarly, in the case of similar multiple quantum H<u>NCA</u> sequence such effect could not be achieved due to more effective relaxation of $^{13}C_\alpha$ nuclei. For larger proteins, however, the cross-correlation effects should be considered and different linewidth for ZQ and DQ spectra might be expected. Comparison of multiple quantum H(N)<u>COCA</u> from Fig. 2A with analogous sequence, depicted in Fig. 2B according to [24], with two separate single quantum evolution periods, is given in Figs. 6D and E. Neglecting, in the first approximation, cross-correlation effects, relaxation rate of DQ/ZQ coherences could be assumed as sum of respective single-quantum relaxation rates. For the same length of t_1 relaxation of DQ/ZQ coherence affects both sequences from Fig. 2 identically, however, sequence 2b is longer by additional period t_1, where SQ-transverse relaxation of $^{13}C'$ spins reduces overall signal amplitude. As it might be expected S/N ratio obtained by longer sequence (Fig. 2B) is reduced, while resolution for MQ-variant is limited only by splittings due to $^{13}C_\alpha-^{13}C_\beta$ couplings. Although, the sensitivity of sequence from Fig. 2B could be improved by constant time $^{13}C'$ evolution, in such a case the maximum t_1 evolution would be limited to ca. 7 ms. Similarly, formally 4D MQ-H<u>NCO-CA</u> technique could be compared with analogous HNC-OCA sequence with three separate evolution periods [27], used in reduced dimensionality manner. When constant time evolution of $^{13}C'$ and ^{15}N would be used, the overall sequence lengths will equal and sensitivity comparable but resolution limited. However, when longer evolution of $^{13}C'$ and or ^{15}N will required the shorter sequence with single MQ-evolution period should be advantageous.

The evolution of multiple quantum coherences is very convenient for measurement of coupling constants with passive spins. The apparent splittings are equal to the sum and difference of couplings with particular nuclei. It is well known that in case when a relatively large coupling is combined with a small one, the accuracy of the latter is improved due to a weaker effect of differential relaxation [28–30]. The proposed techniques, after simple modification, are suitable for the measurement of scalar and residual dipolar couplings, which provide valuable information about protein structure and dynamics [31], and examples of such applications will be presented elsewhere.

All the spectra presented were recorded at 298 K on a Varian Inova 400 spectrometer equipped with a Performa II z-PFG unit and a 5 mm ^1H, ^{13}C, ^{15}N-triple resonance probehead. High power ^1H, ^{13}C, and ^{15}N $\pi/2$ pulses of 6.7, 14.0, and 44.0 μs, respectively, were employed. A sample of 1.5 mM ^{13}C, ^{15}N-labeled ubiquitin in 9:1 H_2O/D_2O at pH 6.0 was used. The experimental details are given in the figure legends. The conventional H<u>NCO</u> sequence with two separate evolution periods was adapted from 3D version implemented in the Varian Userlib ProteinPack package.

3. Conclusions

The application of multiple quadrature rules for multiple quantum spectra allows for full exploitation of the advantages of reduced dimensionality experiments, i.e., short measurement times and resolution limited only by apparent transverse relaxation rates. This kind of experiments is also essential for acquiring tilted projections in reconstruction experiments proposed by [7–10]. The described multiple quantum RD-techniques, due to shorter and simplified pulse sequences, as compared with their single quantum counterparts, are less prone to relaxation loses and RF-pulses imperfections. Additionally, sequences of this type are ideally suitable for scalar or residual dipolar coupling measurements.

References

[1] J. Jeener, Ampere International Summer School II, Basko-Polje, Yugoslavia, 1971.

[2] W.P. Aue, E. Bartholdi, R.R. Ernst, Two-dimensional spectroscopy. Application to nuclear magnetic resonance, J. Chem. Phys. 64 (1976) 2229–2246.

[3] L. Frydman, T. Scherf, A. Lupulescu, The acquisition of multidimensional NMR spectra within a single scan, Proc. Natl. Acad. Sci. USA 99 (2002) 15662–15858.

[4] L. Frydman, A. Lupulescu, T. Scherf, Principles and features of single-scan two-dimensional NMR spectroscopy, J. Am. Chem. Soc. 125 (2003) 9204–9217.

[5] Y. Shrot, L. Frydman, Single-Scan NMR spectroscopy at arbitrary dimensions, J. Am. Chem. Soc. 125 (2003) 11385–11396.

[6] P. Pelupessy, Adiabatic single scan two-dimensional NMR spectrocopy, J. Am. Chem. Soc. 125 (2003) 12345–12350.

[7] Ē. Kupče, R. Freeman, New methods for fast multidimensional NMR, J. Biomol. NMR 27 (2003) 101–113.

[8] Ē. Kupče, R. Freeman, Reconstruction of the three-dimensional NMR spectrum of a protein from a set of plane projections, J. Biomol. NMR 27 (2003) 383–387.

[9] Ē. Kupče, R. Freeman, Projection-reconstruction of three-dimensional NMR spectra, J. Am. Chem. Soc. 125 (2003) 13958–13959.

[10] B.E. Coggins, R.A. Venters, P. Zhou, Generalized reconstruction of n-D NMR spectra from multiple projections: application to the 5-D HACACONH spectrum of protein G B1 domain, J. Am. Chem. Soc. 126 (2004) 1000–1001.

[11] T. Szyperski, G. Wider, J.H. Buschweller, K. Wüthrich, Reduced dimensionality in triple-resonance NMR experiments, J. Am. Chem. Soc. 115 (1993) 9307–9308.

[12] B. Brutscher, J.P. Simorre, M.S. Caffrey, D. Marion, Design of a complete set of two-dimensional triple-resonance experiments for assigning labeled proteins, J. Magn. Reson. B 105 (1994) 77–82.

[13] F. Löhr, H. Rüterjans, A new triple-resonance experiment for the sequential assignment of backbone resonances in proteins, J. Biomol. NMR 6 (1995) 189–197.

[14] K. Ding, A.M. Gronenborn, Novel 2D triple-resonance NMR experiments for sequential resonance assignments of proteins, J. Magn. Reson. 156 (2002) 262–268.

[15] B. Bersch, E. Rossy, J. Coves, B. Brutscher, Optimized set of two-dimensional experiments for fast sequential assignment, secondary structure determination, and backbone fold validation of 13C/15N-labelled proteins, J. Biomol. NMR 27 (2003) 57–67.

[16] W. Koźmiński, I. Zhukov, Multiple quadrature detection in reduced dimensionality experiments, J. Biomol. NMR 26 (2003) 157–166.

[17] S. Kim, T. Szyperski, GFT NMR, a new approach to rapidly obtain precise high-dimensional NMR spectral information, J. Am. Chem. Soc. 125 (2003) 1385–1393.

[18] G. Bodenhausen, R.R. Ernst, The accordion experiment, a simple approach to three-dimensional NMR spectroscopy, J. Magn. Reson. 45 (1981) 367–373.

[19] G. Bodenhausen, R.R. Ernst, Direct determination of rate constants of slow dynamic processes by two-dimensional accordion spectroscopy in nuclear magnetic resonance, J. Am. Chem. Soc. 104 (1982) 1304–1309.

[20] J. Leppert, B. Heise, O. Ohlenschläger, M. Görlach, R. Ramachandran, Triple resonance MAS NMR with (13C, 15N) labelled molecules: reduced dimensionality data acquisition Via 13C-15N heteronuclear two-spin coherence transfer pathways, J. Biomol. NMR 28 (2004) 185–190.

[21] A.G. Palmer III, J. Cavanagh, P.E. Wright, M. Rance, Sensitivity improvement in proton-detected two-dimensional heteronuclear correlation NMR spectroscopy, J. Magn. Reson. 93 (1991) 151–170.

[22] L.E. Kay, P. Keifer, T. Saarinen, Pure absorption gradient enhanced heteronuclear single quantum correlation spectroscopy with improved sensitivity, J. Am. Chem. Soc. 114 (1992) 10663–10665.

[23] M. Sattler, M.G. Schwedinger, J. Schleuchter, C. Griesinger, Novel strategies for sensitivity enhancement in heteronuclear multidimensional NMR experiments employing pulsed firl gradients, J. Biomol. NMR 5 (1995) 11–22.

[24] M. Sattler, J. Schleuchter, C. Griesinger, Heteronuclear multidimensional NMR experiments for the structure determination of proteins in solution employing pulsed field gradients, Prog. NMR Spectrosc. 34 (1999) 93–158.

[25] G. Drobny, A. Pines, S. Sinton, D.P. Weitekamp, D. Wemmer, Fourier transform multiple quantum nuclear magnetic resonance, Faraday Div. Chem. Soc. Symp. 13 (1979) 49–174.

[26] D. Marion, K. Wüthrich, Application of phase sensitive two-dimensional correlated spectroscopy (COSY) for measurements of 1H–1H spin–spin coupling constants in proteins, Biochem. Biophys. Res. Commun. 113 (1983) 967–974.

[27] D. Yang, L.E. Kay, TROSY triple-resonance four-dimensional NMR spectroscopy of a 46 ns tumbling protein, J. Am. Chem. Soc. 121 (1999) 2571–2575.

[28] A. Abragam, Principles of Nuclear Magnetism, Clarendon Press, Oxford, 1961.

[29] A. Rexroth, P. Schimdt, S. Szalma, T. Geppert, H. Schwalbe, C. Griesinger, New principle for the determination of coupling constants that largely suppresses differential relaxation effects, J. Am. Chem. Soc. 117 (1995) 10389–10390.

[30] G. Cornilescu, B.E. Ramirez, M.K. Frank, M. Clore, A.M. Gronenborn, A. Bax, Correlation between 3hJNC′ and hydrogen bond length in proteins, J. Am. Chem. Soc. 121 (1999) 6275–6279.

[31] A. Bax, Weak alignment offers new NMR opportunities to study protein structure and dynamics, Protein Sci. 12 (2003) 1–16.

[32] A.J. Shaka, Composite pulses for ultra-broadband spin inversion, Chem. Phys. Lett. 120 (1985) 201–205.

[33] D.J. States, R.A. Haberkorn, R.J. Ruben, Two-dimensional nuclear overhauser experiment with pure absorption phase in four quadrants, J. Magn. Reson. 48 (1982) 286–292.

[34] D. Marion, M. Ikura, R. Tschudin, A. Bax, Rapid recording of 2D NMR spectra without phase cycling. Application to the study of hydrogen exchange in proteins, J. Magn. Reson. 85 (1989) 393–399.